Biuletyn WAT
Vol. LXI, Nr 4, 2012

Dynamic behaviour of a metallic cylinder striking a rigid target

EDWARD WŁODARCZYK, ADAM JACKOWSKI, MARCIN SARZYŃSKI

Military University of Technology, Faculty of Mechatronics and Aviation,
00-908 Warsaw, 2 Kaliskiego Str., Poland, edward.wlodarczyk@wat.edu.pl

Abstract. The initial-boundary value problem of the one-dimensional dynamical plastic deformation within the scope of large strain of a metallic cylindrical rod has been analytically solved in a closed form. The deformation of the rod has been caused by its normal impact on rigid target. The rod material in the deformed part is defined by incompressible, rigid-plastic, linear strain hardening model. A rigid-plastic, strain hardening material model provided better correlation with experimental data than perfectly-plastic model. The results presented in this paper have applicable values. Derived in the paper, closed analytical relations, written by elementary functions, give researchers and engineers insight into interaction of the physical parameters of the rod during the impact process and post-impact one.
Keywords: dynamics, rod dynamics, Taylor impact, large strains, strain hardening

1. Introduction

The Taylor test was developed by G.J. Taylor and co-workers during the 1940s [1-4] as a method of estimating the dynamic strength of ductile materials in compression. The technique consists of firing a cylinder of the material of interest against a massive, rigid target. The dynamic flow stress can be then found by recovering the deformed cylinder, measuring its change of shape and using adequate formula. There has been much interest in impact testing and estimating dynamic yield stress since then [5-26].

The present view seems to be that Taylor's theory fails to provide reliable yield stress estimates, especially for tests conducted at higher velocities of striking. For these reasons, many investigators are correlating their results with sophisticated computer analyses which are capable of utilizing several complex forms of constitutive equations (e.g. [27, 28]). These programs can match the geometry of a post-test specimen with very high accuracy and give very reliable estimates for material properties. The drawback is that these programs are expensive and often require substantial amounts of time to execute.

The authors of paper [13] assert that simple engineering theories, such as that given by Taylor, still have considerable value. Such theories frequently give investigators insight into the interaction of physical parameters and their relationship to the outcome of the event. These interactions are, more often than not, difficult to ascertain from complex computer outputs. As a result, simple engineering theories often provide the basis for the design of experiments and are frequently used to refine the areas in which computing is to be done.

Recently there has been renewed interest in Taylor impact or its variants [29] as a method of testing constitutive relations [30, 31] for a wide range of materials. One reason for this technique is so useful in testing constitutive models in the wide range of strain rates is that it covers in one experiment from shock loading at the impact face to quasi-static loading at the rear [32, 33]. It also produces large strains at the impact face.

Bearing in mind the above facts, the simple engineering method to determine dynamic mechanical characteristics of the rod during the striking process and post-impact process is presented in this paper. The rod material is approximated by rigid-plastic, linear strain hardening model. For such a type of material, closed forms of the analytical formulae for determining all dynamic parameters of the rod have been derived. The formulae are written by means of elementary functions. The theoretical results, obtained in this paper are compatible to experimental data. Similar problems were studied numerically in [15] and [34].

2. Formulation of the problem

Consider the initial-boundary value problem: a cylindrical flat-ended metallic rod strikes normally on a rigid flat target. The initial velocity of the rod is denoted by U, and its initial dimensions are: the length denoted as L and the cross-sectional area as F_0. For enough large value of the velocity U, a portion of the rod placed at a target face is deformed plastically. As in other problems of plasticity, it may be permissible to neglect elastic strains in comparison with plastic strains, particularly within the scope of the large plastic strains. Bearing in mind this fact, it is assumed that the rod material is rigid-plastic, linear strain hardening, and incompressible into a region of plastic strains. Making this assumption is equivalent to supposing that the hind part of the rod, not reached by the plastic wave front at any instant, behaves as a rigid body. This assumption leads to a considerably simplified solution of the plastic flow resulting from impact.

The conditions of the considered problem are as shown in Fig. 1. The rigid back part of the rod is approaching to target with the absolute velocity u. The plastic wave front is propagated away from the impact surface with the absolute velocity υ, leaving the material behind it at rest since elastic recovery is neglected. These are absolute velocities, and due to this the solution is not being carried out explicitly in terms of Lagrange co-ordinates. F and σ are the cross-sectional area and nominal stress just behind the plastic wave front, and F_0 and σ_{sd} just ahead of it; σ_{sd} is the dynamic yield stress since the material ahead of the wave front is about to become plastic; ρ is the density of the rod material.

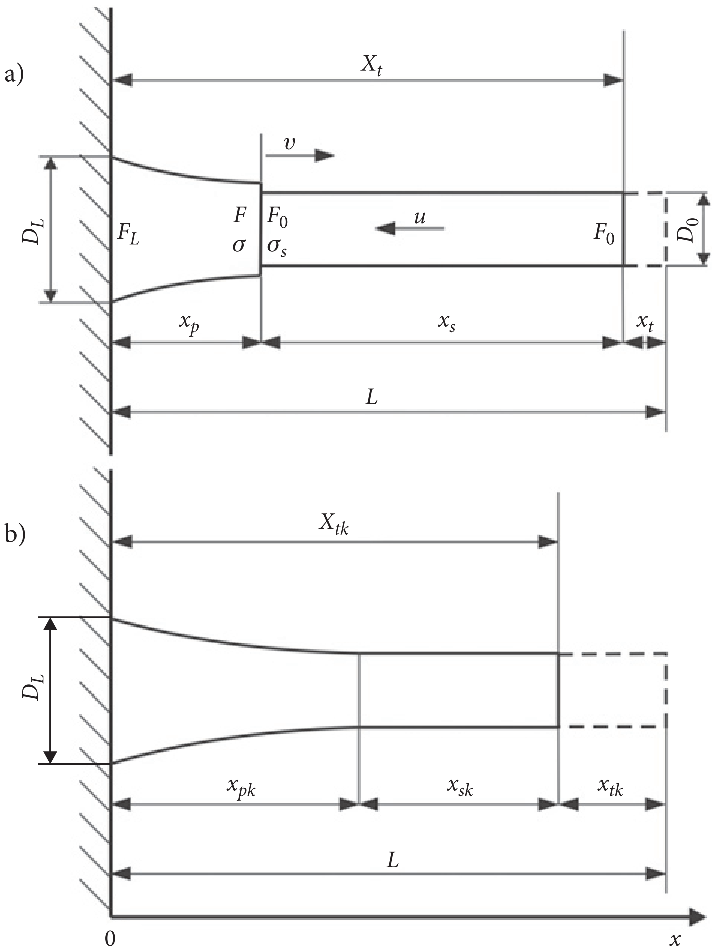

Fig. 1. Forms of deformation on which rigid-plastic solution is based: (a) during deformation, (b) after deformation

The remaining symbols, shown in Fig. 1, denote:
x_p is the momentary length of deformed part of the rod,
x_s is the momentary length of undeformed part of the rod,
x_t is the momentary displacement of the rear end of the rod,
X_t is the total momentary length of the rod.

Additionally, the index k denotes the final values of the quoted above parameters of post-impact, e.g. x_{pk} is the final length of deformed part of the rod, and so on.

Neglecting compressibility in the plastic deformed material, the equation of continuity takes the form

$$(u+v)F_0 = vF. \tag{2.1}$$

This leads to the following expression for the longitudinal compressive strain behind the plastic wave front

$$\varepsilon = \frac{F-F_0}{F} = \frac{u}{u+v}. \tag{2.2}$$

Defining x_s as the undistorted length at any instant, we have

$$\frac{dx_s}{dt} = -(u+v). \tag{2.3}$$

Momentum balance across the wave front yields the equation

$$\rho(u+v)u = \sigma - \sigma_{sd}, \tag{2.4}$$

because when the wave front passes through the distance $dx_s = -dt(u+v)$, the velocity of this element becomes zero ($u = 0$).

The equation of motion of the rigid part of the rod is

$$\rho x_s \frac{du}{dt} = -\sigma_{sd}. \tag{2.5}$$

The stress-strain curve of the rod material is approximated by the linear expression (broken line in Fig. 2)

$$\sigma - \sigma_{sd} = E_w \varepsilon, \tag{2.6}$$

where E_w = constant is the modulus of linear strain hardening. It is assumed that the material behaviour is rate-independent, $\sigma = \sigma(\varepsilon)$, and rigid-plastic, that is why elastic strains are negligible, similarly to [1-3].

By means of expression (2.6) one can approximate the stress-strain curves of high-strength alloy-steels [15], with accuracy sufficient for technical purposes.

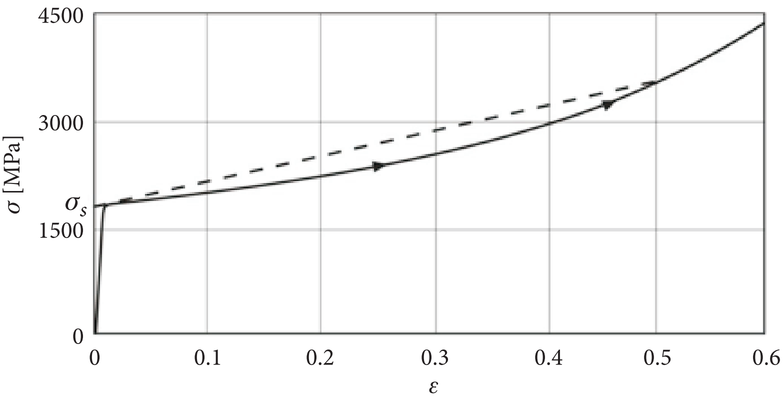

Fig. 2. Assumed static stress-strain curve in compression of Ni – Cr steels [15]; under consideration the rod material is represented by the broken line; σ and ε denote the nominal stress and the nominal strain, respectively

Such a formulated problem, completed by initial and boundary conditions (see sec. 3), has been solved in the analytical form in the next section of this paper.

3. Analytical solution of the problem

Straightforward algebraic transformations of relationships (2.2), (2.4), and (2.6) yield

$$u = c\varepsilon \, , \tag{3.1}$$

$$v = c(1-\varepsilon) \, , \tag{3.2}$$

where

$$c = \sqrt{\frac{E_w}{\rho}} \, . \tag{3.3}$$

From formulae (3.1) and (3.2) it follows that

$$u + v = c = \text{constant}. \tag{3.4}$$

Then, integrating Eq. (2.3) and using of the initial condition $x_s = L$ for $t = 0$ give:

$$x_s = L - ct \, . \tag{3.5}$$

So, the length of the rigid part of the rod x_s decreases proportionally to time.

In turn, Eq. (2.5) and relation (3.5), and the initial condition in the form $u = U$ for $t = 0$, after integrating yield

$$u(t) = U + \frac{\sigma_{sd}}{\rho c} \ln\left(1 - \frac{ct}{L}\right). \tag{3.6}$$

From expressions (3.4) and (3.6) it follows that the propagation velocity of the plastic wave front $\upsilon(t)$ increases in course of time according to relation

$$\upsilon(t) = c - u(t) = c - U - \frac{\sigma_{sd}}{\rho c} \ln\left(1 - \frac{ct}{L}\right). \tag{3.7}$$

Therefore, according to (3.7) and (3.6), the plastic wave velocity υ increases from $(c\text{-}U)$ to c.

In papers [1-3] it has been assumed that υ = constant during the whole impact process. It is far-reaching simplification and is not in accordance with reality.

Condition $u(t_k) = 0$ and expression (3.6) determine the instant t_k ending the striking process, namely

$$\ln\left(1 - \frac{ct_k}{L}\right) = -\frac{\rho c U}{\sigma_{sd}},$$

or

$$t_k = \frac{L}{c}\left[1 - \exp\left(-\frac{\rho c U}{\sigma_{sd}}\right)\right]. \tag{3.8}$$

In agreement with relationships (3.5) and (3.8), the final length of rigid part of the rod is

$$x_{sk} = L \exp\left(-\frac{\rho c U}{\sigma_{sd}}\right) = L \exp\left(-\frac{\sqrt{\rho E_w}}{\sigma_{sd}} U\right). \tag{3.9}$$

Of formula (3.9), it follows that the final length x_{sk} for given rod material (ρ, σ_{sd}, E_w), decreases exponentially with increasing the striking velocity U; if $U \to \infty$, then $x_{sk} \to 0$. It is non-real case. Because real value of the velocity U is limited, usually $U < c$, the rigid part of the rod preserves (Fig. 3).

From formula (3.9), after transformation, we obtain

$$\sigma_{sd} = \frac{\sqrt{\rho E_w} U}{\ln(L/x_{sk})}. \tag{3.10}$$

So, measuring the post-impact final length x_{sk} in the deformed rod for given value of the impact velocity U one may to estimate the dynamic yield stress of material by means of relation (3.10).

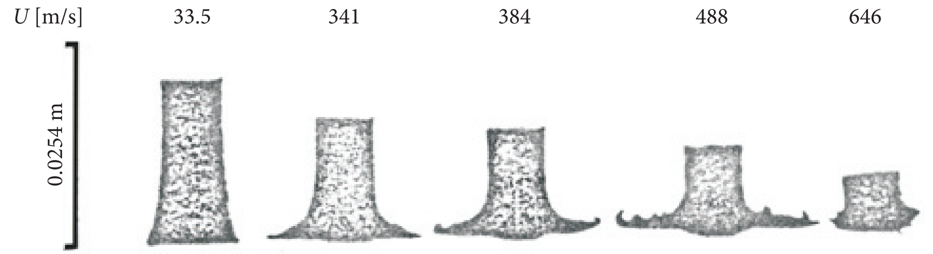

Fig. 3. Steel cylinders after test [3]

Displacement of the end of the undeformed part rod is defined by formula

$$x_t = \int_0^t u(\tau)d\tau = \int_0^t \left[U + \frac{\sigma_{sd}}{\rho c} \ln\left(1 - \frac{c\tau}{L}\right)\right] d\tau = \\ = Ut - \frac{\sigma_{sd}}{E_w} L \left[\left(1 - \frac{ct}{L}\right) \ln\left(1 - \frac{ct}{L}\right) + \frac{ct}{L}\right]. \tag{3.11}$$

In turn, the length of the deformed part of the rod is determined by expression

$$x_p(t) = \int_0^t v(\tau)d\tau = L - \left[x_s(t) + x_t(t)\right] = \\ = \left[c\left(1 + \frac{\sigma_{sd}}{E_w}\right) - U \right] t + L \frac{\sigma_{sd}}{E_w} \left(1 - \frac{ct}{L}\right) \ln\left(1 - \frac{ct}{L}\right). \tag{3.12}$$

The all quoted above parameters, defining the dynamics of the rod during striking, are expressed explicitly by means of analytical time-dependent elementary functions. Let x denote the Lagrangian coordinate aligned with the axis of the rod and having its origin in the impact plane (Fig. 1). Then, the Lagrangian coordinate, x, defining the place of plastic wave front on the plane (x, t) amount:

$$x(t) = L - x_s(t) = ct\ , \tag{3.13}$$

where

$$0 \le t \le t_k; \quad 0 \le x \le ct_k.$$

According to formulae (3.1) and (3.6), the strain ε is defined by the function

$$\varepsilon(t) = \frac{u(t)}{c} = \frac{U}{c} + \frac{\sigma_{sd}}{E_w} \ln\left(1 - \frac{ct}{L}\right) = \frac{U}{c} + \frac{\sigma_{sd}}{E_w} \ln \frac{x_s(t)}{L}\ . \tag{3.14}$$

From analysis of relation (3.14) it follows that

$$\varepsilon_{\max} = \varepsilon(0) = \frac{U}{c} = U \Big/ \sqrt{\frac{E_w}{\rho}} \ . \tag{3.15}$$

Differentiation of the function $\varepsilon(t)$ with respect to t yields

$$\frac{d\varepsilon}{dt} = \dot{\varepsilon}(t) = -\frac{\sigma_{sd}}{E_w}\frac{c}{L-ct} = -\frac{\sigma_{sd}}{E_w}\frac{c}{x_s(t)} \ . \tag{3.16}$$

It is seen that the absolute value of the strain rate, $|\dot{\varepsilon}|$, changes in the range

$$|\dot{\varepsilon}_{\min}| = \frac{\sigma_{sd}}{E_w}\frac{c}{L} \leq |\dot{\varepsilon}(t)| \leq \frac{\sigma_{sd}}{E_w}\frac{c}{x_{sk}} = |\dot{\varepsilon}_{\max}| \ . \tag{3.17}$$

From expressions: (2.2), (3.1), (3.2), and (3.14) after simple transformations we obtain the formula defining the current diameter of the deformed part of the rod $D_p(t)$, namely

$$D_p(t) = \frac{D_0}{\sqrt{1-\varepsilon(t)}} = D_0\left[1 - \frac{U}{c} - \frac{\sigma_{sd}}{E_w}\ln\left(1-\frac{ct}{L}\right)\right]^{-\frac{1}{2}}, \tag{3.18}$$

where D_0 denotes the initial diameter of the rod.

The analysis of the function $D_p(t)$ by means of formula (3.18) gives:

$$D_{p\max}(t) = D_p(0) = D_L = D_0\left(1-\frac{U}{c}\right)^{-\frac{1}{2}} \ . \tag{3.19}$$

The maximal diameter $D_{p\max}$ intensively increases as increases the striking velocity U, and for $U \to c$ is $D_{p\max} \to \infty$. It is non-real case, because earlier striking end of the rod is crumbled. This fact is corroborated by the experimental results (Fig. 3).

4. Example

Let us consider a uniform chromium-nickel steel rod of the initial dimensions, length $L = 0.0127$ m (0.5 in.) and the diameter $D_0 = 0.008636$ m (0.34 in.). Mechanical parameters of the steel are as follows: the density $\rho = 7800$ kg/m^3, the static nominal yield strength $\sigma_s = R_{0.2} = 1800$ MPa, and the strain-hardening modulus $E_w = 3500$ MPa. Assumed stress-strain curve in compression for this steel is depicted in Fig. 2. The calculations were performed for the following values of the striking velocity: U = 196 m/s, U = 266 m/s, and U = 300 m/s using experimental results depicted in Fig. 4 [15].

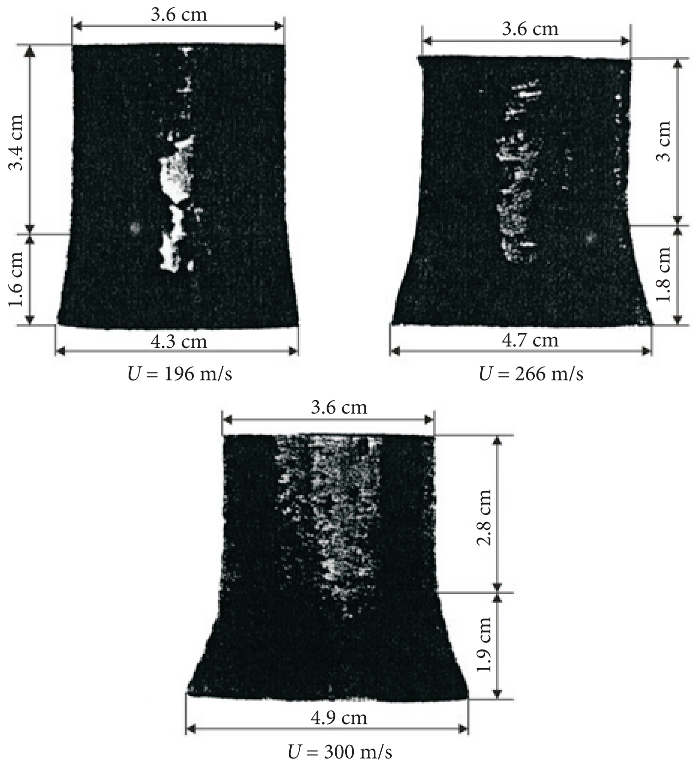

Fig. 4. Shape of cylinders after Taylor test [15]. (All cylinders were originally: D_0 = 0.008636 m (0.34 in.), L = 0.0127 m (0.5 in.))

Depicted in Fig. 4 dimensions of the photograms of the deformed cylinders are given in the scale of 1:0.24. The initial length of the cylinder is L= 5.3 cm in this scale.

Computational results of the selected parameters, characterizing dynamics of the tested steel rod during Taylor's impact at some striking velocities are listed in Table 1.

Table 1

Computational results of the selected parameters for chromium-nickel steel rod during Taylor's test in assumed at time points t

<table>
<tr><td colspan="2">$t \cdot 10^6$ [s]</td><td>0</td><td>2</td><td>4</td><td>6</td><td>$t_k \cdot 10^6 = 6.8$</td><td></td></tr>
<tr><td rowspan="12">$U = 196$ m/s</td><td>ct/L</td><td>0</td><td>0.105</td><td>0.211</td><td>0.316</td><td>0.358</td><td></td></tr>
<tr><td>x_s/L</td><td>1</td><td>0.894</td><td>0.789</td><td>0.683</td><td>0.641</td><td></td></tr>
<tr><td>x_t/L</td><td>0</td><td>0.027</td><td>0.045</td><td>0.055</td><td>0.056</td><td></td></tr>
<tr><td>x_p/L</td><td>0</td><td>0.079</td><td>0.166</td><td>0.262</td><td>0.303</td><td></td></tr>
<tr><td>D_p/D_0</td><td>1.189</td><td>1.132</td><td>1.076</td><td>1.022</td><td>1</td><td></td></tr>
<tr><td>$\varepsilon = u/c$</td><td>0.293</td><td>0.220</td><td>0.137</td><td>0.042</td><td>0</td><td></td></tr>
<tr><td>v/c</td><td>0.707</td><td>0.780</td><td>0.863</td><td>0.958</td><td>1</td><td></td></tr>
<tr><td>$\varepsilon_{\max}$</td><td colspan="6">0.293</td></tr>
<tr><td>$\dot{\varepsilon}_{\min} \cdot 10^{-4}$ [s^{-1}]</td><td colspan="6">3.4765</td></tr>
<tr><td>$\dot{\varepsilon}_{\max} \cdot 10^{-4}$ [s^{-1}]</td><td colspan="6">5.4192</td></tr>
<tr><td>σ_{sd} [MPa]</td><td colspan="6">2307</td></tr>
<tr><td>$\sigma_{\max}$ [MPa]</td><td colspan="6">3330</td></tr>
<tr><td colspan="2">$t \cdot 10^6$ [s]</td><td>0</td><td>2</td><td>4</td><td>6</td><td>8</td><td>$t_k \cdot 10^6 = 8.23$</td></tr>
<tr><td rowspan="12">$U = 266$ m/s</td><td>ct/L</td><td>0</td><td>0.105</td><td>0.211</td><td>0.316</td><td>0.422</td><td>0.434</td></tr>
<tr><td>x_s/L</td><td>1</td><td>0.894</td><td>0.789</td><td>0.683</td><td>0.578</td><td>0.566</td></tr>
<tr><td>x_t/L</td><td>0</td><td>0.038</td><td>0.067</td><td>0.086</td><td>0.094</td><td>0.094</td></tr>
<tr><td>x_p/L</td><td>0</td><td>0.068</td><td>0.144</td><td>0.231</td><td>0.328</td><td>0.340</td></tr>
<tr><td>D_p/D_0</td><td>1.288</td><td>1.212</td><td>1.141</td><td>1.073</td><td>1.007</td><td>1</td></tr>
<tr><td>$\varepsilon = u/c$</td><td>0.397</td><td>0.319</td><td>0.232</td><td>0.132</td><td>0.015</td><td>0</td></tr>
<tr><td>v/c</td><td>0.603</td><td>0.681</td><td>0.768</td><td>0.868</td><td>0.985</td><td>1</td></tr>
<tr><td>$\varepsilon_{\max}$</td><td colspan="6">0.397</td></tr>
<tr><td>$\dot{\varepsilon}_{\min} \cdot 10^{-4}$ [s^{-1}]</td><td colspan="6">3.6804</td></tr>
<tr><td>$\dot{\varepsilon}_{\max} \cdot 10^{-4}$ [s^{-1}]</td><td colspan="6">6.5020</td></tr>
<tr><td>σ_{sd} [MPa]</td><td colspan="6">2442</td></tr>
<tr><td>$\sigma_{\max}$ [MPa]</td><td colspan="6">3832</td></tr>
</table>

cont. Table 1

	$t \cdot 10^6$ [s]	0	2	4	6	8	$t_k \cdot 10^6 = 8.94$
$U = 300$ m/s	ct/L	0	0.105	0.211	0.316	0.422	0.472
	x_s/L	1	0.894	0.789	0.683	0.578	0.528
	x_t/L	0	0.043	0.078	0.102	0.115	0.117
	x_p/L	0	0.063	0.133	0.215	0.307	0.355
	D_p/D_0	1.346	1.259	1.180	1.105	1.033	1
	$\varepsilon = u/c$	0.448	0.370	0.282	0.181	0.063	0
	υ/c	0.552	0.630	0.718	0.819	0.937	1
	ε_{max}	0.448					
	$\dot{\varepsilon}_{min} \cdot 10^{-4}$ [s^{-1}]	3.7020					
	$\dot{\varepsilon}_{max} \cdot 10^{-4}$ [s^{-1}]	7.0074					
	σ_{sd} [MPa]	2456					
	σ_{max} [MPa]	4024					

In turn, Fig. 5 shows the calculated longitudinal compressive plastic strain ε versus independent variable (ct/L) for some selected values of the impact velocity U.

After a Taylor test, the compressive strain ε in the plastic deformation zone of the rod decreases with a distance from the impact face. It has the maximum values, $\varepsilon_{max} = \varepsilon(0)$, at the impact face, which increases directly proportionally to the impact

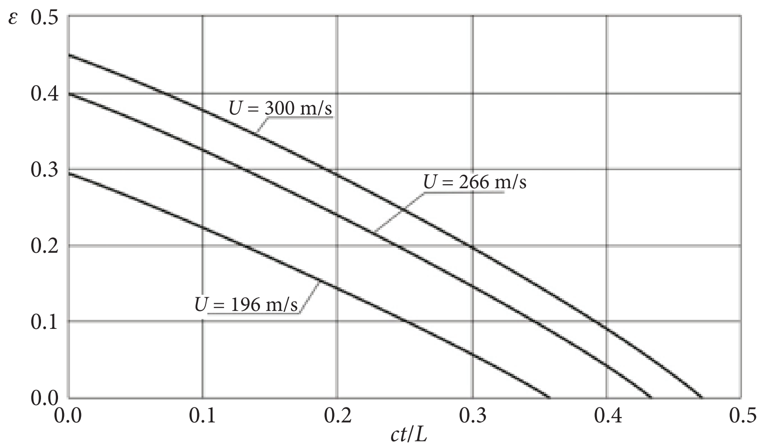

Fig. 5. The calculated plastic strain ε versus variable (ct/L) for some selected values of the impact velocity U

velocity U (3.15). The strain $\varepsilon(t_k) = 0$ at the interface between the deformed and undeformed sections of the rod, i.e. in the following cross-sections: $x_{pk} = 0.302L$ for $U = 196$ m/s, $x_{pk} = 0.340L$ for $U = 266$ m/s, $x_{pk} = 0.355L$ for $U = 300$ m/s.

Variations of the dimensionless absolute velocities $v(t)/c$ and $u(t)/c$ versus the non-dimensional time ct/L for some selected values of the impact velocity U are depicted in Fig. 6. Figure 6 shows that displacement velocity of the rigid part rod $u(t)$ monotonically decreases according to the logarithmic functions from the maximal value, $u_{\max} = U$, at the impact face ($t = 0$) and is zero at the interface between the deformed and undeformed sections of the rod at the instant $t = t_k$ (3.8). The plastic wave velocity $v(t)$, on the contrary to the velocity $u(t)$, increases according to this some logarithmic function from the minimal value, $v_{\min} = v(0) = c - U$, at the contact face ($t = 0$) and reaches the maximum $v_{\max} = c$ at the instant $t = t_k$ (3.8).

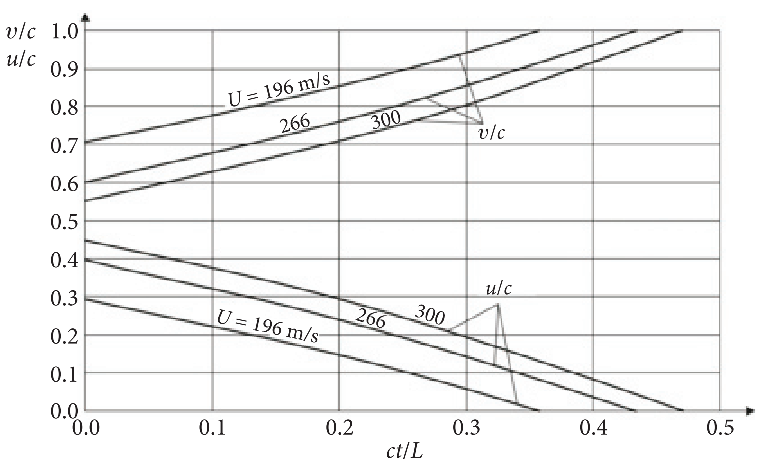

Fig. 6. The changes of the relative absolute velocities $v(t)/c$ and $u(t)/c$ versus (ct/L) for some values U

The variations of the non-dimensional length of the deformed part rod, $x_p(t)/L$, versus non-dimensional time, ct/L, for some values of the impact velocity U are depicted in Fig. 7. As it can be seen, the dimensionless quantity, $x_p(t)/L$, is zero at the impact face and increases to the maximal value $\overline{x}_{pk} = x_p(t_k)/L$ which reaches at the interface between the deformed and undeformed section of the rod at instant $t = t_k$, namely: $\overline{x}_{pk} = 0.302$ for $U = 196$ m/s, $\overline{x}_{pk} = 0.340$ for $U = 266$ m/s and $\overline{x}_{pk} = 0.355$ for $U = 300$ m/s. Note that together with the increase in the impact velocity U, the increment $\Delta\overline{x}_{pk}$ of the functions $x_p(t_k)/L$ decreases to zero (broken line in Fig. 7). For $U \to c$, the deformed end of the rod is being crushed during striking (Fig. 3).

The final shapes of the deformed rods after Taylor's test obtained by means of theoretical computations for some values of the impact velocity U are depicted in Fig. 8. The obtained shapes of the deformed rods are conformable to experimental data presented in papers [3] and [15] (Fig. 4).

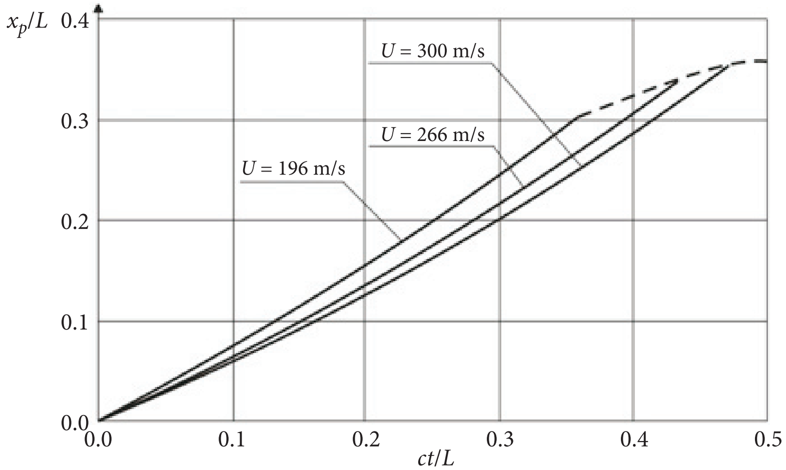

Fig. 7. The calculated dimensionless length $x_p(t)/L$ versus the variable ct/L for some values of the velocity U

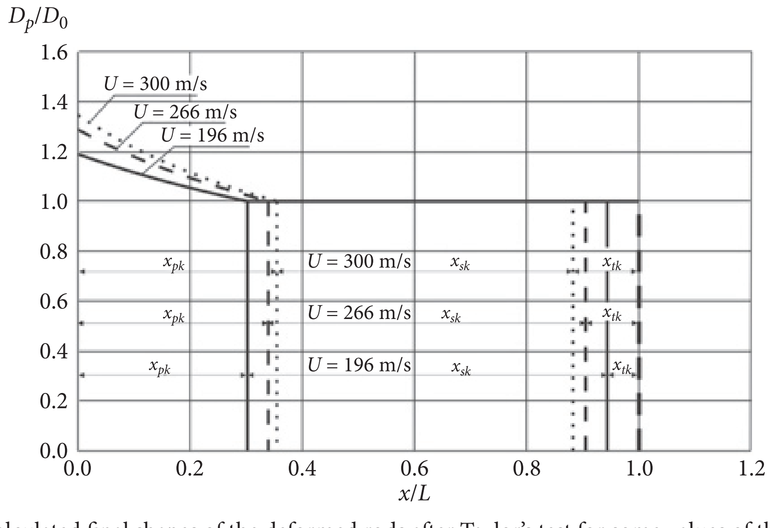

Fig. 8. Calculated final shapes of the deformed rods after Taylor's test for some values of the impact velocity U

5. Conclusions

The general conclusion from this study is that for plastic strains large compared with elastic strains, the rigid-plastic type of analysis provides a satisfactory and simple analytical method. For the rod with linear strain-hardening striking a rigid target (Taylor test), by means of this model, interesting results have been obtained in this paper, namely:

1. The longitudinal compressive strain ε in the plastic deformation zone of the rod monotonically decreases with a distance from the impact face. It has the maximum value
2.

$$\varepsilon_{\max} = \varepsilon(0) = \frac{U}{c} = U \Big/ \sqrt{\frac{E_w}{\rho}}$$

at the impact face and is zero at the interface between the deformed and undeformed sections of the rod (Fig. 4).

3. The absolute value of the strain-rate changes during the striking process in the range

$$\left|\dot{\varepsilon}_{\min}\right| = \frac{\sigma_s}{E_w}\frac{c}{L} \le \left|\dot{\varepsilon}(t)\right| \le \frac{\sigma_s}{E_w}\frac{c}{x_{sk}} = \left|\dot{\varepsilon}_{\max}\right| .$$

4. The length of the deformed part of the rod x_p is limited, and independently from a value of the impact velocity U it does not contain the whole rod. The length of the rigid portion of the rod amounts

$$x_{sk} = L\exp\left(-\frac{\sqrt{\rho E_w}}{\sigma_{sd}}U\right).$$

5. For rigid-plastic with linear strain hardening material of the rod, the sum of absolute velocity of the plastic wave $\upsilon(t)$ and absolute velocity of the rigid part of rod $u(t)$ is constant, namely

$$\upsilon(t) + u(t) = c = \sqrt{\frac{E_w}{\rho}} .$$

Numerical calculations placed in paper [15] corroborate this fact.

6. The diameter of the deformed part of rod reaches maximum in the cross-section $x = 0$ contacting with surface of the target, and is equal to

$$D_{p\max}(x) = D_p(0) = D_L = D_0\left(1 - \frac{U}{c}\right)^{-\frac{1}{2}} .$$

At large striking velocity $U \approx c$ deformed end of the rod is crushed (Fig. 3).

7. By means of simple formula (3.10)

$$\sigma_{sd} = \frac{\sqrt{\rho E_w}}{\ln\left(L/x_{sk}\right)}U$$

one can estimate a value of dynamic yield strength for the given material (ρ, E_w) of the rod. For this purpose it is necessary to measure the parameter x_{sk} of the rod after Taylor's test at the given striking velocity U.

8. For plastic strains large compared with elastic strains, the rigid-plastic type of analysis provides a satisfactory and simple analytical method. It gives theoretical results to be compatible with experimental data.
9. Rigid-plastic model of the rod material makes possible the extension of presented here analysis to the case of material with nonlinear strain hardening. We are going to consider this problem in the next paper.

Received April 04 2012, revised June 2011.

REFERENCES

[1] G.I. Taylor, *The testing of materials at high rates of loadin*g, J. Inst. Civ. Eng., 26, 1946.

[2] G.I. Taylor, *The use of flat-ended projectiles for determining dynamic yield stress*, I. *Theoretical considerations*, Proc. Roy. Soc., Series a, London, 194, 1948, 289.

[3] A.C. Whiffin, *The use flat-ended projectiles for determining dynamic yield stress*, II. *Tests on various metallic materials*, Proc. Roy. Soc., Series a, London, 194, 1948, 300.

[4] W.E. Carrington, M.L.V. Gayler, *The use flat-ended projectiles for determining yield stress*, III. *Changes in microstructure caused by deformation at high striking velocities*, Proc. Roy. Soc., Series a, London, 194, 1948, 323.

[5] J.D. Cinnamon, S.S. Jones, J.C. Foster, P.P. Gillis Jr, *An analysis of early time deformation rate and stress in the Taylor impact test. Mechanical Behaviour of Materials*, VI. Proc. of the Sixth Int. Materials Conf., eds. M. Jano. and T. Inouc, Kyoto, Japan, 1, July 1991, 337.

[6] N. Cristescu, *Dynamic plasticity*, North-Holland, Amsterdam, 1967.

[7] J.C. Foster, P.J. Maudlin Jr, S.E. Jones, *On the Taylor test*, Part I: *A continuum analysis of plastic wave propagation*, Proc. of the 1995 APS Topical Conf.: An Shock Compression of Condensed Matter, Seattle, Washington, August 1995, 291.

[8] J.B. Hawkyard, D. Easoton, W. Johnson, *The mean dynamic yield strength of cooper and low carbon steel at elevated temperatures from measurements of the "mushrooms" of flat-ended projectiles*, Int. J. Mech. Sci., 10, 1968, 929.

[9] J.B. Hawkyard, *A theory for the mushrooming of flat-ended projectiles impinging on a flat rigid anvil*, *using energy considerations*, Int. J. Mech. Sci., 11, 1963, 313.

[10] I.M. Hutchings, *Estimation of yield stress in polymers at high strain-rates using G.I. Taylors impact technique*, J. Mech. Phys. Solids, 26, 1979, 289.

[11] G.R. Johnson, T.J. Holmquist, *Evaluation of cylinder-impact test data for constitutive model constants*, J. Appl. Phys., 64, 1988, 3901.

[12] S.E. Jones, P.P. Gillis, J.C. Foster, L.X. Wilson Jr, *A one-dimensional two-phase flow model for Taylor impact specimens*, J. Engr. Mat'ls. Tech., ASME, 113, 1991, 228.

[13] S.E. Jones, P.P. Gillis, J.C. Foster Jr, *On the equation of motion of the undeformed section of a Taylor impact specimen*, J. Appl. Phys., 61, 1987, 499.

[14] S.E. Jones, P.J. Maudlin, P.P. Gillis, J.C. Foster Jr, *An analytical interpretation of high strain rate materials behaviour during early time plastic deformation in the Taylor impact test*, Computers in Engineering, ed. G.A. Gabriele, 2, ASME, New York, 1992, 173.

[15] E.H. Lee, S.J. Tupper, *Analysis of plastic deformation in a steel cylinder striking a rigid target*, J. Appl. Mech., Trans. ASME, 21, 1954, 63.

[16] P.J. Maudlin, J.C. Foster Jr, S.E. Jones, *An engineering analysis of plastic wave propagation in the Taylor test*, Int. J. Impact Engng, 19, 1997, 95.

[17] P.J. Maudlin, J.C. Foster Jr, S.E. Jones, *On the Taylor test*, Part III: *A continuum mechanics code analysis of plastic wave propagation*, Los Alamos National Laboratory report LA-12836-MS, November 1994.

[18] P.J. Maudlin, R.F. Davidson, R.J. Henninger, *Implementation and assessment of the mechanical-threshold-stress model using the EPIC2 and PINON computer codes*, Los Alamos National Laboratory report LA-11895-MS, September 1990.

[19] M.A. Meyers, *Dynamic behaviour of materials*, John Wiley and Sons, INC, New York-Chester-Brisbane-Toronto-Singapore, 1994.

[20] T.C.T. Ting, *Impact of a nonlinear viscoplastic rod on a rigid wall*, J. Appl. Mech. Trans. ASME, 33, 1966, 505.

[21] L.L. Wilson, J.W. House, M.E. Nixon, *Time resolved deformation from the cylinder impact test AFATL-TR-89-76*, November 1989.

[22] E. Włodarczyk, A. Starczewska, J. Materniak, J. Janiszewski, W. Koperski, *Estimation of dynamic yield stress of shell steels by means of the Taylor impact test* (in Polish), Bull, Acad., 1, 56, 2007, 113.

[23] S.E. Jones, P.J. Maudlin, J.C. Forster, *An engineering analysis of plastic wave propagation in the Taylor test*, Int. J. Impact Engng, 19, 2, 1997, 95-105.

[24] S. Kaliski, Cz. Rymarz, K. Sobczyk, E. Włodarczyk, *Waves*, PWN, Warsaw, Elsevier, Amsterdam-Oxford-New York-Tokyo, 1992.

[25] P.G. Shewmon (ed.), V.F. Zackay, *Response of metals to high velocity deformation*, Interscience Publishers, New York-London, 1961.

[26] J.A. Zukas, T. Nicholas, H. Swift, L.B. Greszczuk, D.R. Curran, *Impact dynamics*, John Wiley and Sons, INC, New York-Chester-Brisbane-Toronto-Singapore, 1981.

[27] H.E. Konokman, M.M. Coruh, A. Kayran, *Computational and experimental study of high-speed impact of metallic Taylor cylinders*, Acta Mech., 220, 2011, 61-85.

[28] D.J. Allen, W.K. Rule, S.E. Jones, *Optimizing material strength constants numerically extracted from Taylor impact data*, Experimental Mechanics, 37, 3, 1997.

[29] J.E. Field, S.M. Walley, W.G. Proud, H.T. Goldrein, C.R. Siviour, *Review of experimental techniques for high rate deformation and shock studies*, Int. J. Impact Engineering, 30, 2004, 725-75.

[30] P.J. Maudlin, G.T. Gray Iii, C.M. Cady, G.C. Karcher, *High-rate material modeling and validation using the Taylor cylinder impact test*, Phil. Trans. R. Soc. a, London, 357, 1999, 1707-29.

[31] S.M. Walley, P.D. Church, R. Townsley, J.E. Field, *Validation of a path-dependent constitutive model for FCC and BCC metals using symmetric Taylor impact*, J. Phys. IV, France, 10, 2000, 69-74.

[32] D.D. Radford, G.R. Willmott, S.M. Walley, J.E. Field, *Failure mechanisms in ductile and brittle materials during Taylor impact*, J. Phys. IV, France, 110, 2003, 687-92.

[33] P.D. Church, T. Andrews, B. Goldthorpe, *A review of constitutive model development within DERA*, [in:] Jerome D.M. editor, *Structures under extreme loading conditions*, PVP, vol. 394, New York: American Society of Mechanical Engineers, 113-20.

[34] D. Raftopoloulos, N. Davids, *Elastoplastic impact on rigid targets*, AJAA Journal, 5, 12, 1967, 2254-60.

E. WŁODARCZYK, A. JACKOWSKI, M. SARZYŃSKI

Dynamiczne zachowanie się metalowego walca uderzającego w sztywną tarczę

Streszczenie. Rozwiązano analitycznie jednowymiarowe zagadnienie dynamicznej deformacji, z dużymi odkształceniami plastycznymi metalowego cylindrycznego pręta, uderzającego prostopadle w sztywną tarczę. Materiał pręta modelowano w strefie odkształceń plastycznych nieściśliwym ośrodkiem sztywno-plastycznym z liniowym wzmocnieniem. Sztywno-plastyczny model z liniowym wzmocnieniem zapewnia dobrą korelację wyników teoretycznych z eksperymentalnymi i w sposób istoty upraszcza rozwiązanie problemu. Zdaniem autorów, wyniki prezentowane w pracy mają aplikacyjne walory. Wyprowadzone zamknięte analityczne relacje, zapisane elementarnymi funkcjami dają badaczom i inżynierom bezpośredni wgląd we wzajemne oddziaływania między parametrami pręta podczas procesu zderzenia i po jego zakończeniu.

Słowa kluczowe: dynamika, dynamika pręta, test Taylora, duże odkształcenia, wzmocnienie odkształceniowe